

# XIANELLA: A NEW MAT-FORMING CALCIFIED CYANOBACTERIUM FROM THE MIDDLE–LATE ORDOVICIAN OF NORTH CHINA

by JEONG-HYUN LEE<sup>1</sup> and ROBERT RIDING<sup>2</sup>

<sup>1</sup>Department of Geology and Earth Environmental Sciences, Chungnam National University, Daejeon, 34134, Korea; jeonghyunlee@cnu.ac.kr

<sup>2</sup>Department of Earth and Planetary Sciences, University of Tennessee, Knoxville, TN 37996, USA; rriding@utk.edu

Typescript received 28 March 2016; accepted in revised form 25 May 2016

**Abstract:** *Xianella hongii* gen. et sp. nov. is described from the Middle–Late Ordovician of Shaanxi, China and interpreted as a calcified cyanobacterial sheath. *Xianella* filaments formed cable-like strands that constructed thick fenestral layers. The specimens occur in metre-sized limestone blocks, possibly derived from local collapse of a reefal platform margin. In combination with micrite, some of which is intraclastic and peloidal, *Xianella* created thick and extensive stacks of layered calcified fenestral fabric that appear to be syngedimentarily calcified open-frame mat

deposits. The fenestrae range from small, laminose and very irregular, to large equidimensional areas ~2 cm across. Fenestrae with rounded outlines resemble primary gas bubbles observed in present-day microbial mats. These delicate fabrics are comparable in structure and quality of preservation with those of some Proterozoic silicified stromatolitic mats.

**Key words:** *Xianella* gen. nov., cyanobacteria, calcified microbe, China, Ordovician.

SMALL calcareous tubular filaments often interpreted as *in vivo* calcified cyanobacterial sheaths (Pollock 1918; Riding 1977, 2006), that first appear in the Proterozoic (Klein *et al.* 1987), are widely distributed and locally common in Phanerozoic marine carbonates (Riding 2012). The best known calcified genus, *Girvanella*, first described from the Ordovician, typically occurs as loosely tangled filaments (Nicholson & Etheridge 1878), but long and relatively straight forms also occur, such as *Cladogirvanella*, first described from the Triassic (Ott 1966). From the Ordovician of China we describe *Xianella*, a new genus consisting of unbranched filaments. Like *Cladogirvanella* it forms thick anastomosing cable-like strands, but *Xianella* is significantly larger than *Cladogirvanella* and exhibits overall subhorizontal orientation relative to the substrate with an open mat-like structure in which the strands commonly surround millimetric to centimetric pore-spaces, some of which are rounded and resemble gas bubbles. The *Xianella* filaments are commonly coated by peloidal micritic patches and veneers that resemble calcified biofilm, and the tangled filaments enclose numerous fenestrae. These features suggest that *Xianella* was a key component of thick calcified porous microbial mats. These deposits are unusual in creating macroscopic wavy fenestra-rich structures that extend throughout breccia blocks up to 2 m across. Syngedimentary calcification and

early cementation preserved fine filament details, as well as the variously erect and prostrate orientations of the cable-like strands that define numerous large and small fenestrae. We are unaware of similar calcified fabrics on this scale, but these extensive *Xianella* mats can be compared with silicified cyanobacterial mats in Proterozoic stromatolites and Palaeozoic spring deposits (Krings *et al.* 2007), some of which resemble present-day examples (Knoll & Golubic 1992, fig. 1). The detail preserved in these *Xianella* mat deposits is unexpectedly good; reflecting a combination of *in vivo* sheath calcification and syngedimentary cementation, sufficient to conserve the outlines of gas-bubble fabric. Detailed study of *Xianella* mats may help us further understand the nature of ancient microbial mats and the conditions affecting their formation.

## GEOLOGICAL SETTING AND METHOD

During the Ordovician, the Sino-Korean (North China) Block was either a microcontinent near the margin of Gondwana (Li & Powell 2001) or part of Gondwana itself (McKenzie *et al.* 2011), and accumulated shallow-marine sediments (Meng *et al.* 1997). The Ordovician succession in this southern part of the block contains reefs which

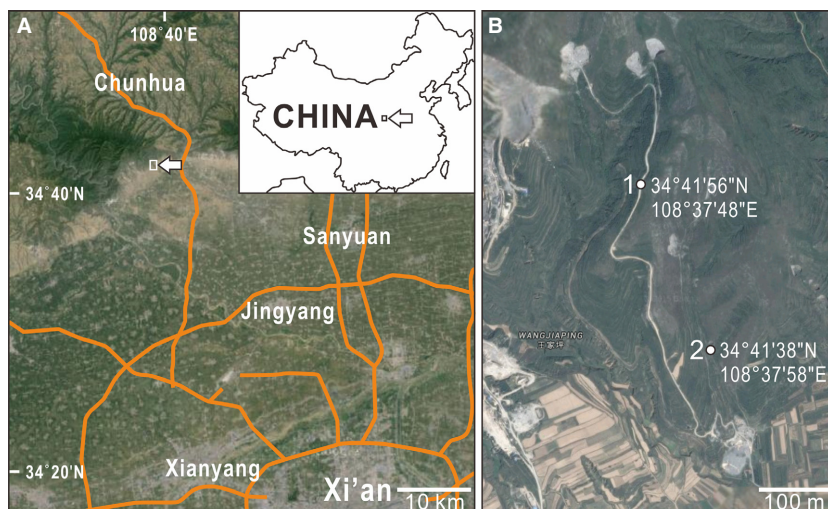


**FIG. 1.** Study area in north central Shaanxi Province in north central China. A, satellite map of central Shaanxi Province with location of *Xianella* samples (arrow), 60 km NNW of Xi'an city. B, satellite map showing Locality 1 (road section) and Locality 2 (quarry) where *Xianella* samples were collected. Colour online.

developed during the Middle–Late Ordovician (Ye *et al.* 1995; Webby 2002, p. 149; Wang *et al.* 2012; Jiang *et al.* 2013).

Samples were collected from the Tiewadian area on the southwestern side of the Ordos Basin in Jingyang County, 60 km NNW of the centre of Xi'an, Shaanxi Province, China (Fig. 1). These outcrops are road and quarry sections located on the southern slope of the mountains 6 km west of Kouzhen, adjacent to the area of the tomb of the Tang Emperor Xuānzong. In the area sampled these are represented by the Upper Ordovician Beiguoshan Formation (Fig. 2), consisting of more than 180 m of coarse angular limestone breccia blocks up to 3 m in size, although the majority are pebble to small boulder in size (Fig. 3A). Thin shale and lime mudstone horizons locally define bedded units within the breccia that are ~1–5 m thick. Stromatactoid geopetal fabrics show that the large block in Fig. 3A is on its side. The blocks consist of a variety of lithotypes (peloidal packstone/grainstone, skeletal packstone/wackestone).

Fossils reported from breccia blocks in the Tiewadian section include *Amsassia*, *Cryptolichenaria*, *Forolinia*, *Phacelophyton*, *Renalcis*, *Girvanella*, *Ortonellina*, *Nuia*, *Vermiporella* and *Proaulopora* (Ye *et al.* 1995) and *Lichenaria*, *Rhabdotetradium*, *Syringoporella*, *Catenipora*, *Quepora*, *Yaoxianopora*, *Parastelliporella*, *Plasmoporella*, *Dinophyllum*, *Ningnanophyllum* and *Favistella* (Jiang *et al.* 2013). Overall, these assemblages broadly suggest shallow marine conditions of Middle–Late Ordovician age. Ye *et al.* (1995) regarded the breccia as an essentially *in situ* reef deposit, but most blocks are broken and displaced and appear to be allochthonous gravity flow/slope talus deposits, probably from a carbonate platform margin (Gao & Peng 2006; Jiang *et al.* 2013). These Tiewadian breccias were originally attributed to

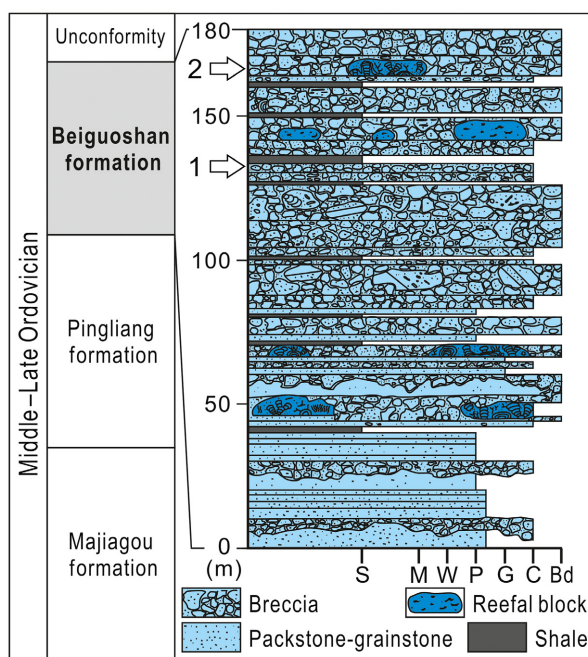


**FIG. 2.** Stratigraphy of study area (courtesy of J. Park). Samples were collected from Localities 1 and 2 (horizons arrowed) in the Middle–Late Ordovician coarse breccia-dominated Beiguoshan Formation. Colour online.

the Pingliang Formation (Ye *et al.* 1995; Gao & Peng 2006), but have subsequently been ascribed to the Beiguoshan Formation (Cao *et al.* 2011; Jiang *et al.* 2013). A Middle (Ye *et al.* 1995) or Late (Cao *et al.* 2011; Jiang *et al.* 2013) Ordovician age has been suggested for this deposit (see Sun *et al.* 2014 for regional stratigraphy).

The samples of *Xianella* described here were collected from breccia blocks of the Beiguoshan Formation at two different horizons ~40 m vertically apart, at two different

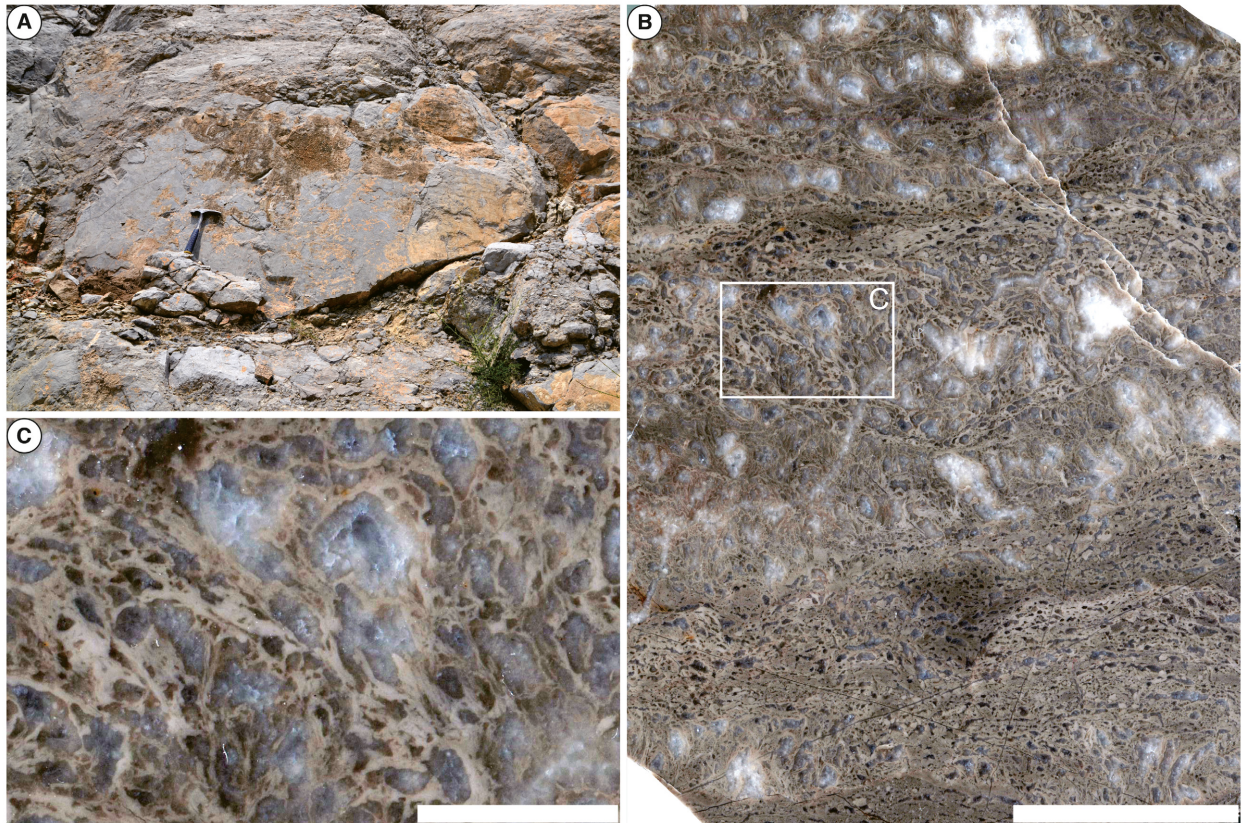


**FIG. 3.** A, Beiguoshan breccia outcrop showing a large block (marked by hammer) surrounded by smaller limestone fragments; stromatolite-like fabrics indicate that the large block is on its side with its top to the left. B, polished slab of *Xianella* boundstone (from Locality 1) showing numerous sub-millimetric to centimetric fenestrae (NIGPAS159413). C, detail of area in B with anastomosing *Xianella* strands defining irregular millimetric spar-filled fenestrae. Scale bars represent 4 cm (B); 1 cm (C). Colour online.

localities within the section (Fig. 2); polished slabs and thin sections of the microbial carbonates were prepared. The samples from these localities are similar. Those illustrated here are from Locality 1; the sample is from a single block ~40 cm across, consisting entirely of *Xianella* filaments with a distinctive fenestral fabric (Fig. 3B, C). On the other hand, Locality 2 contains a block ~2 m across, which appears to consist entirely of *Xianella* fabric. Microscale measurements of *Xianella* filament and bundle dimensions were made from photomicrographs. Numerical dimensions of fenestrae were measured using 'ImageJ' (Schneider *et al.* 2012).

## SYSTEMATIC PALAEOONTOLOGY

### Cyanobacteria

#### Genus XIANELLA nov.

*Derivation of name.* After Xi'an, the regional capital city of Shaanxi.

*Type species.* *Xianella hongii* sp. nov., by monotypy.

*Diagnosis.* Calcareous microfossil; narrow unbranched tubular filaments forming prostrate and erect anastomosing cable-like strands; wall micritic.

*Comparisons.* We interpret *Xianella* as the calcified sheath of a relatively large filamentous cyanobacterium. This is consistent with interpretations of *Girvanella* and similar genera (Bornemann 1886; Hinde 1887, pp. 227–228; Pollock 1918, p. 255; Pia 1927, p. 38; Frémy & Dangeard 1935; Riding 1975, 1977). *Xianella* is large relative to *Cladogirvanella* and most *Girvanella* species, but is similar in size to sheaths of some extant cyanobacteria, particularly those with multiple trichomes, e.g. *Microcoleus* or Proterozoic *Eomicrocoleus* (Horodyski & Donaldson 1980, fig. 15; Schopf 1996; Seong-Joo & Golubic 1999). Putative calcified filaments of sulphur bacteria are not tubular and show distinctive bending of the filaments suggesting looping behaviour (e.g. Oliveri *et al.* 2010); these features do not resemble *Xianella*.

*Remarks.* The organization of *Xianella* into relatively thick anastomosing cable-like strands most closely resembles *Cladogirvanella* Ott, 1966 from the Ladinian (Middle Triassic) of the Italian Dolomites. Ott's (1966) suggestion that *Cladogirvanella* tubes may bifurcate remains unconfirmed. *Xianella* is distinguished from *Cladogirvanella* by its larger tube size and the overall prostrate alignment of its cable-like strands. In the type-species of *Cladogirvanella*, *C. cipitensis*, tubes are typically 4–6 µm in internal diameter and form multi-filament cable-like strands 0.1–0.4 mm in diameter that are erect and radial (Ott 1966). Some *Xianella* cable-like bundles of tubes are erect, but these mainly form connections between equally or more abundant prostrate and arcuate *Xianella* layers and bundles, in complex trellis-like lattice-works that can extend for several tens of centimetres.

Bundled filamentous structure also occurs in *Subtifloria* Maslov, 1956, and the similar genera *Botominella* Reitlinger, 1959 and *Batinevia* Korde, 1966, all best known from the Cambrian. But none of these appear to form long branched cables, although they may be fragments. This marked difference in length, together with the generally more parallel alignment of their fine filaments, distinguish *Subtifloria*, *Botominella* and *Batinevia* from both *Cladogirvanella* and *Xianella*.

Cambrian *Razumovskia* Krasnopeeva, 1937 forms prostrate, thin, felted layers with upturned ends, and short vertical tangled to curved tufts and outgrowths that arise from its upper surface. These details distinguish it from *Xianella*. Ordovician *Acuasiphonoria* Liu *et al.*, 2016 also consists of arrays of elongate filaments. Its long gently curved tubes are described as pointed and possibly branched at acute angles (Liu *et al.* 2016); these features, as well as its lack of anastomosed bundles, distinguish *Acuasiphonoria* from *Xianella*.

*Xianella hongii* sp. nov.

Figures 4–7

*Derivation of name.* After Jongsun Hong, who helped discover this fossil.

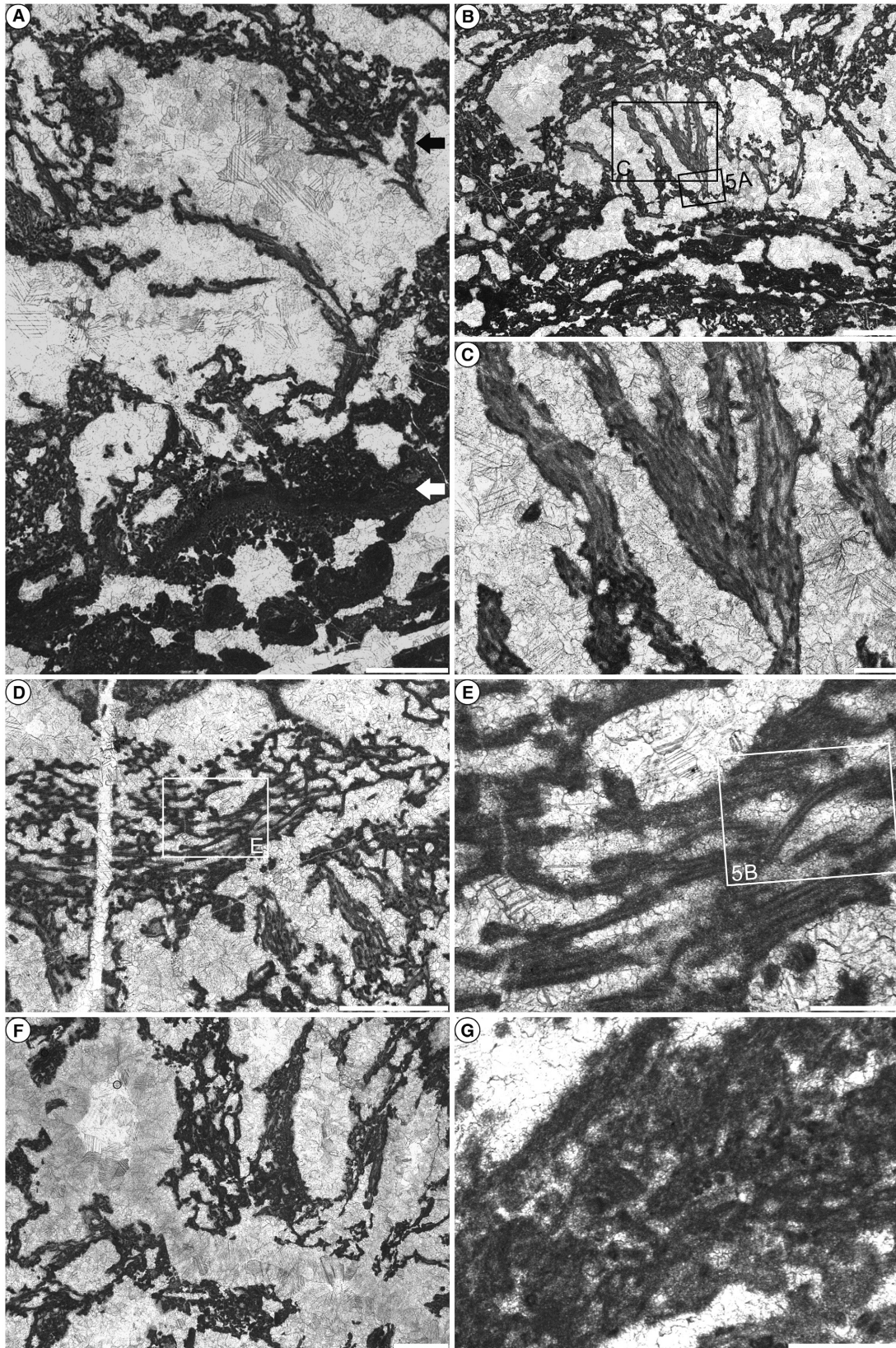
*Type specimen.* Specimens are housed at the Nanjing Institute of Geology and Palaeontology under repository numbers NIGPAS159413 (holotype; slab) and NIGPAS159414–159419 (paratypes; thin sections).

*Type locality.* Two localities of downslope transported reefal blocks in the Beiguoshan Formation, Tiewadian section, Shaanxi Province, China (34°41'56"N/108°37'48"E, 34°41'38"N/108°37'58"E). Middle–Late Ordovician.

*Diagnosis.* As for genus.

*Description.* Filaments, straight to sinuous, interlaced into cable-like strands forming an open anastomosing network in which layers of prostrate strands, joined by more erect branched strands, define relatively large spar-filled areas (Figs 3C, 4A–C). Tube diameter 20–60 µm; wall thickness 4–12 µm (Figs 5, 6); tubes commonly extend 200–400 µm in length (Fig. 4D, E). The tubes form anastomosing cable-like strands 0.1–2.0 mm (commonly 150–700 µm) in width, in which individual filaments range from closely adjacent to up to 30 µm apart, and can enclose spar-filled cavities 100–200 µm in width and up to ~1 mm long (Fig. 4C, F). These areas of fenestrae and *Xianella* cables often lie between much denser horizons dominated by irregular laterally elongate fenestrae up to 1 mm high and 3 mm wide (Fig. 4A), or by denser micrite areas, locally with a fragmented intraclast-like structure (Fig. 4A). In these crudely layered successions, the cable-like strands often form complex lattice-works enclosing large, irregular to rounded spar-filled fenestrae up to 2 cm (commonly ~3 mm) across (Figs 3C and 7). These open lattice-works retain a layered structure with distinct layers of prostrate filaments, which can be separated by 5–10 mm or more, and are connected by widely spaced erect strands (Fig. 7B, C). Locally, some of the large fenestrae defined by *Xianella* filaments have distinctly rounded margins (Fig. 7). These porous *Xianella*-dominated frameworks (Fig. 3B) form deposits up to at least 40 cm, and possibly more than 1 m, in width. In the denser horizons, the relatively small spar-filled laterally elongate fenestrae (Fig. 7A) occupy up to ~35% of

**FIG. 4.** Thin section photographs of *Xianella hongii* (from Locality 1). A, typical overall mat fabric (NIGPAS159414); the dense micrite–intraclast–peloidal lower part, with local mainly prostrate *Xianella* (white arrow), passes up into more erect *Xianella* strands defining large fenestrae (black arrow). B, fabric similar to A with medium-size fenestrae (central area) bounded by bundles of *Xianella* filaments (NIGPAS159415). C, detail of B showing erect cable-like strands formed by bundles of *Xianella* filaments; bundles in the centre branch upward. D, bundles and aligned clusters of subvertical (lower right) and prostrate (centre) *Xianella* filaments, associated with relatively large fenestrae (NIGPAS159416). E, detail of sub-horizontal *Xianella* filaments in D, showing unbranched tubes with uniform diameters and micritic walls; irregular thin surficial veneers on the outer surfaces of the tubes may be calcified biofilm. F, anastomosing *Xianella* cables defining medium to large fenestrae filled or lined by cloudy cement (NIGPAS159416); the central part of the large fenestra to the upper left was subsequently infilled by clear blocky cement. G, clotted micrite containing diffuse peloids, poorly defined filaments, and scattered transverse sections of *Xianella* tubes (NIGPAS159416). Scale bars represent 1 mm (A, B, D, F); 0.2 mm (C, E, G).



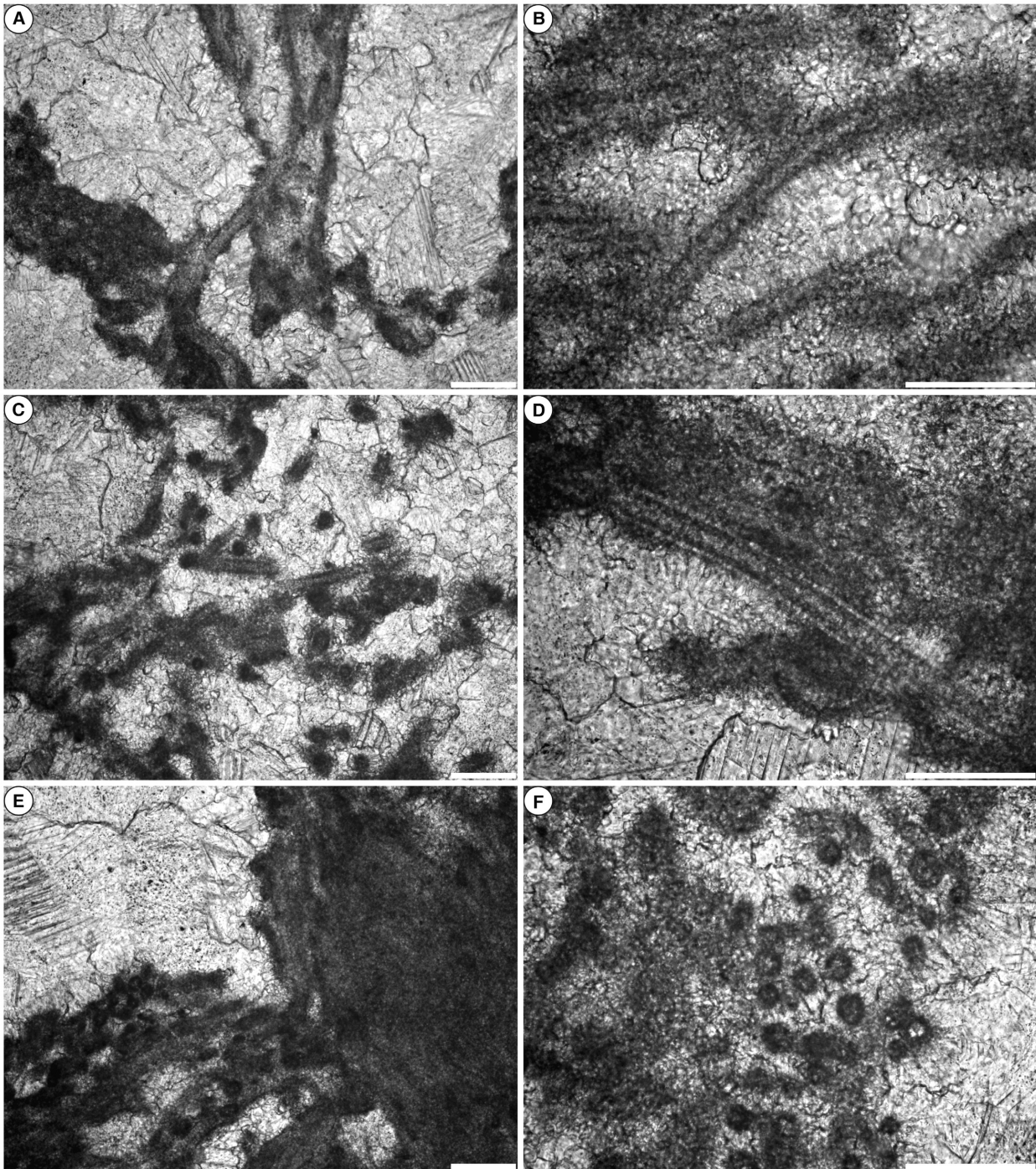


**FIG. 5.** Close up photographs of *Xianella hongii* (from Locality 1). A–C, longitudinal sections of tubes; A, NIGPAS159415; B, NIGPAS159416; C, NIGPAS159417. D, rare occurrence of a hyaline-like sparitic wall (NIGPAS159417). E, margin of the lower part of the large fenestra (upper left) illustrated in Fig. 9A, showing densely aggregated diffuse tubes paralleling the fenestra margin (NIGPAS159416). F, transverse sections of tubes (NIGPAS159417). All scale bars represent 0.1 mm.

the fabric (Fig. 8A), whereas the more open frameworks, with sub-vertical strands and sub-horizontal layers that define large rounded vugs (Fig. 7B, C), are up to 70% or more spar-filled (Fig. 8B, C).

*Remarks.* The specimens are from breccia fragments and blocks whose source remains uncertain. The associated shallow water fossils (Ye *et al.* 1995; Jiang *et al.* 2013) would be consistent with toe-of-slope collapse breccias

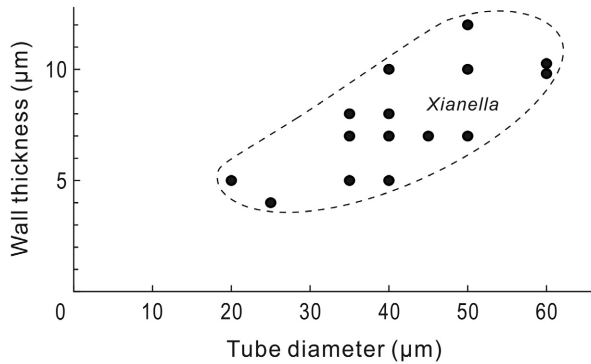


FIG. 6. Dimensions of *Xianella hongii* filaments.

from a carbonate platform margin that could have included reef constructions. This setting is comparable with that of Middle Triassic *Cladogirvanella*, originally described from allochthonous blocks (Cipit Boulders) in the Italian Dolomites (Ott 1966). Upward change from denser, micritic areas with smaller fenestrae (Fig. 7A) to less dense areas with erect *Xianella* filaments (Fig. 7B), suggests cyclic repetition that could reflect changes in *Xianella* mat growth and/or accretion.

## MICROBIAL MAT STRUCTURE

*Xianella* filaments are commonly coated by thin irregular micritic patches and veneers that resemble calcified biofilm (Figs 4E, 5D). Tangled strands of filaments are locally associated with patches of diffuse micrite patterned by faint peloids and scattered microspar fenestrae. Larger areas and layers of inhomogeneous micrite, such as those in the lower part of Fig. 4A, contain very thin slightly aligned curved fenestrae and resemble amalgamated compacted layers of intraclasts and masses of mud-grade carbonate. These horizons also contain sporadic filaments similar to those that form *Xianella* but generally not arranged in bundles.

Both large and small spaces between the *Xianella* filaments and strands are either filled or lined by cloudy cement, and the filaments are generally aligned parallel to the margin of the fenestrae (Figs 4, 5D). This arrangement is similar to the present-day example figured by Mata *et al.* (2012, fig. 5a). In addition to a thick marginal layer of cloudy cement, the central parts of the larger Tiewadian fenestrae are filled by larger clear blocky cement crystals (Fig. 4F). We interpret this association of fabrics as lithified microbial mats in which growth cavities were initially synsedimentarily cemented by cloudy cement, and then infilled by clear burial cement. We infer that *Xianella* sheaths could have been calcified *in vivo*, allowing them to maintain an open meshwork structure

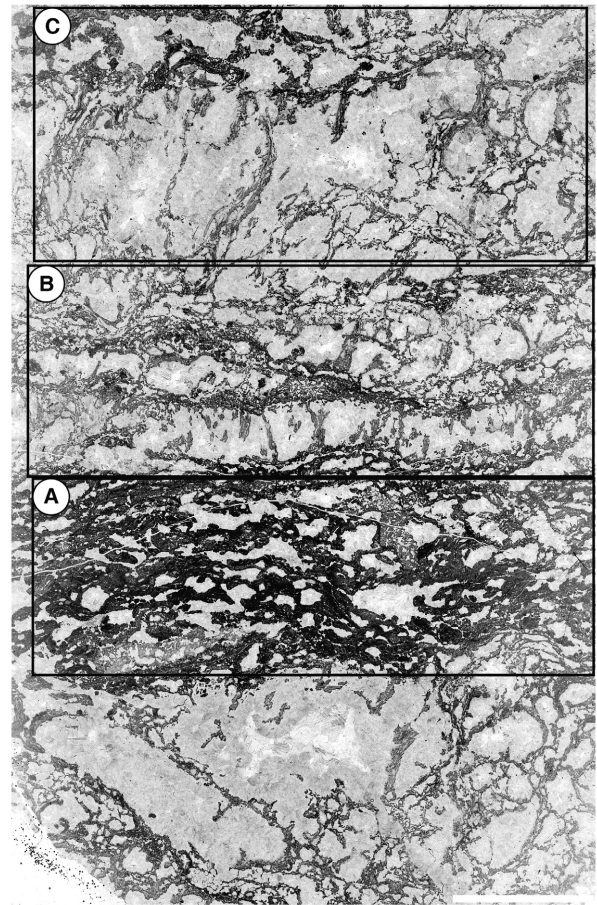
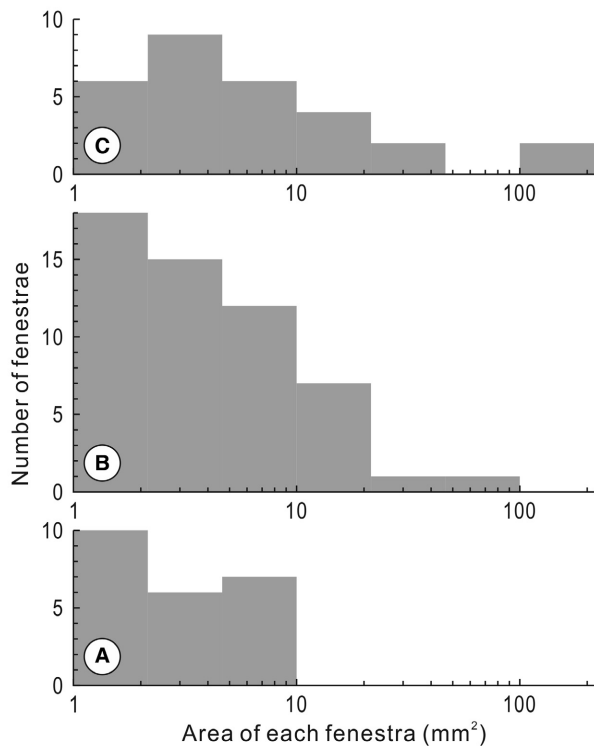


FIG. 7. Thin-section of *Xianella* boundstone (Locality 1) showing successive upward changes in fenestral fabric (NIG-PAS159417). The size and areal percentage of fenestrae generally increases upwards from A to C. A, dense area dominated by diffuse clotted peloidal micrite with small laterally elongate spar-filled fenestrae; B, mid-sized fenestrae bounded by prostrate and also erect *Xianella* bundles; C, large fenestrae, some of which are centimetric, defined by variously oriented bundles of *Xianella* filaments. Most fenestrae are filled or lined by cloudy cement, with clear cement occupying the centres of larger fenestrae. Note that the lowest, unnumbered, part of the thin-section is similar in fabric to that of part C, and examination of larger areas (e.g. Fig. 3B) indicates vertical repetition in mat structure. Scale bar represents 1 cm.

that locally incorporated fine sediment. Early lithification by the cloudy blocky cements would have supported the open meshwork fabric. The name *Xianella* refers just to the filamentous fossil.

Broadly comparable mat structures are locally preserved by early silicification in Proterozoic stromatolites and Palaeozoic spring deposits (Krings *et al.* 2007). Proterozoic examples include filamentous cyanobacterial sheaths such as *Siphonophycus* (Schopf 1968; Yun 1981; Knoll 1985, fig. 8; Knoll *et al.* 1989, 2013; Seong-Joo &



**FIG. 8.** Comparison of fenestra size in areas A–C of Figure 7, measured using ImageJ. Fenestrae smaller than 1 mm<sup>2</sup> are not included. Each bar represents a fenestra size in the range  $\log(1/3)$ . Overall, fenestra size increases from A to C.

Golubic 1999; Sergeev 2001; Cao & Yin 2011) and *Eomicrococleus* (Horodyski & Donaldson 1980; Awramik *et al.* 1985; Kumar & Srivastava 1995). Some of these open meshworks of silicified filaments closely resemble present-day examples (Knoll & Golubic 1992, fig. 1). They can also show associations of vertical and horizontal filament alignment (Golubic & Focke 1978; Knoll & Golubic 1992, fig. 1; Seong-Joo & Golubic 1998, figs 2a, 12), some of which are reminiscent of *Xianella* fabrics in overall dimensions and organization (Seong-Joo & Golubic 1999; Knoll *et al.* 2013).

Knoll *et al.* (2013, fig. 11) contrasted Mesoproterozoic examples of thin-filament mats containing abundant primary void space, with adjacent laminated mats containing few primary voids. They compared them with present-day mats at Laguna Mormona (Horodyski & Vonder Haar 1975) and noted that these kinds of depositional fabrics became less common in Neoproterozoic successions. Whereas Knoll *et al.* (2013, fig. 9a) observed that open mat structure is preserved better in silicified areas than in carbonate, Tiewadian *Xianella* mats are both calcified and uncompacted. They therefore show that the quality of porous mat structure preservation by early carbonate lithification could locally, in the Middle–Late Ordovician, be comparable to that of silicification. Presumably this required not only *in vivo* sheath calcification but also symsedimentary lithification of surrounding fabrics. The peloidal micrites observed at Tiewadian are less clearly

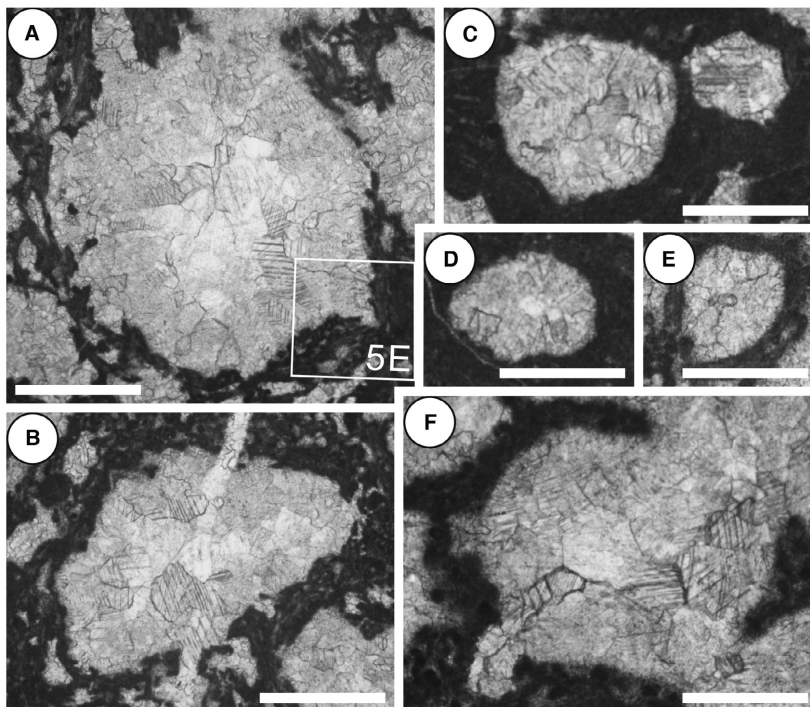


**FIG. 9.** Examples of sub-rounded fenestrae ~0.5–2 mm in size. A, B, E, NIGPAS159416; C, D, F, NIGPAS159418. Scale bars represent 1 mm (A, B); 0.5 mm (C–F).

defined than some other fossil examples (Riding & Tomás 2006), but it remains possible that they too might be products of bacterial calcification or bacterial sulphate reduction (cf. Visscher *et al.* 2000; Guido *et al.* 2014).

**Rounded cavities.** *Xianella* fenestral deposits have a macroscopic wavy structure, defined by subtle colour banding and large, often vertically extended, voids (Fig. 3B, C), some of which have smooth rounded margins (Fig. 9A–F). These are mainly sub-millimetric to millimetric in size.

Mats of filamentous microbes such as cyanobacteria commonly create distinctive morphologies, e.g. ridges and tufts produced by trichome gliding, phototaxis and cohesion (e.g. Walter *et al.* 1976; Shepard & Sumner 2010). Additional three-dimensional structuring can arise from production of gas bubbles (Mata *et al.* 2012) which can also contribute to the development of coniform lamination (Bosak *et al.* 2009, 2010). Experiments with modern microbial mats have shown that sub-millimetric to millimetric oxygen bubbles can persist within mats for weeks to months (Bosak *et al.* 2010). Methane can also form bubbles that are similar to the rounded fenestrae in *Xianella* mats. Examples from modern gas hydrates also display similar sized rounded fabrics formed by methane bubbles (Brewer *et al.* 1997; Suess *et al.* 1999, fig. 2d). It should also be noted that bubbles not only occupy, but can expand, mat-cavities by stretching and locally disrupting networks of organic material. It is therefore possible that the rounded fenestrae present in *Xianella* mats, which are similarly millimetric in size (Fig. 9), could have been formed by cyanobacterially-generated oxygen bubbles. Mat disruption would also account for local stretching and discontinuity in these porous fabrics (Fig. 4A). In addition, early dissolution and/or bioerosion can enlarge fenestra margins (e.g. Riding & Zhuravlev 1995, fig. 3c). However, we have not observed clear evidence for this in our *Xianella* samples, and filaments typically parallel fenestra margins without showing truncation (Fig. 5E). Syntsedimentary lithification promoted preservation of these structures.

## CONCLUSIONS

*Xianella* is a mat forming calcified cyanobacterium from the Middle–Late Ordovician near Xi'an, North China. It occurs in breccia block deposits that may have been derived by local collapse of a reefal platform margin. *Xianella* consists of narrow, unsegmented and unbranched tubes interpreted as *in vivo* calcified sheaths, intertwined to form branched and anastomosed cable-like strands enclosing originally open, now spar-filled, fenestrae. In combination with micrite, some of which is intraclastic and peloidal, *Xianella* created thick and extensive calcified fenestral sheets, which we interpret as syntsedimentarily

calcified open-frame mat fabrics. Fenestrae within these deposits range from small, laminose and very irregular to large and more equidimensional. Some fenestrae have rounded outlines with resemblances to primary gas bubbles. The structure and affinities of *Xianella* are most similar to mid-Triassic *Cladogirvanella*, which also occurs in allochthonous margin-derived blocks. However, *Cladogirvanella* differs from *Xianella* in having much thinner tubes and a distinctly erect radiating growth form. *Xianella* shows that Middle–Late Ordovician microbial syntsedimentary bioinduced calcification could preserve delicate mat structures comparable to those observed in early silicified Proterozoic stromatolitic mats.

**Acknowledgements.** JHL thanks D.-J. Lee, J. Hong, J. Park, S.-J. Choh, and K. Liang for help in fieldwork and sample preparation. J. Hong noticed *Xianella* in the field and J. Park helped with figure preparation. JHL was supported by the Basic Science Research Program of the National Research Foundation of Korea (2015R1A6A3A03019727). We thank reviewers for comments on an early version of the manuscript, *Papers in Palaeontology* reviewers for helpful suggestions, and Lesley Cherns and Sally Thomas for excellent editing. This study is a contribution to IGCP Project 653 'The onset of the Great Ordovician Biodiversity Event'.

## DATA ARCHIVING STATEMENT

Data for this study are available in the Dryad Digital Repository: <http://dx.doi.org/10.5061/dryad.2nh26>

*Editor.* Lesley Cherns

## REFERENCES

- AWRAMIK, S. M., McMENAMIN, D. S., YIN, C., ZHAO, Z., DING, Q. and ZHANG, S. 1985. Prokaryotic and eukaryotic microfossils from a Proterozoic/Phanerozoic transition in China. *Nature*, **315**, 655–658.
- BORNEMANN, J. 1886. Die Versteinerungen des Cambrischen Schichtensystems der Insel Sardinien nebst vergleichenden Untersuchungen über analoge Vorkommnisse aus anderen Ländern I. *Nova Acta der Kaiserslichen Leopoldinisch-Carolinischen Deutschen Akademie der Naturforscher*, **51**, 1–147.
- BOSAK, T., LIANG, B., SIM, M. S. and PETROFF, A. P. 2009. Morphological record of oxygenic photosynthesis in conical stromatolites. *Proceedings of the National Academy of Sciences*, **106**, 10939–10943.
- BUSH, J. W., FLYNN, M. R., LIANG, B., ONO, S., PETROFF, A. P. and SIM, M. S. 2010. Formation and stability of oxygen-rich bubbles that shape photosynthetic mats. *Geobiology*, **8**, 45–55.
- BREWER, P. G., ORR, F. M. Jr, FRIEDERICH, G., KVENVOLDEN, K. A., ORANGE, D. L., McFARLANE, J. and KIRKWOOD, W. 1997. Deep-ocean field

- test of methane hydrate formation from a remotely operated vehicle. *Geology*, **25**, 407–410.
- CAO, R. and YIN, L. 2011. Microbiota and microbial mats within ancient stromatolites in South China. 65–86. In TEWARI, V. C. and SECKBACH, J. (eds). *Stromatolites: interaction of microbes with sediments*. Springer, 752 pp.
- CAO, J.-Z., FENG, Q., ZHAO, W., ZHOU, S.-C., WANG, Q.-Y., LIU, Z., LU, Y.-J. and LI, Y.-L. 2011. Sequence stratigraphy of Ordovician strata in the south part of Ordos Area. *Acta Sedimentologica Sinica*, **29**, 286–292. [in Chinese with English abstract]
- FRÉMY, P. and DANGEARD, L. 1935. Sur la position systématique des Girvanelles. *Bulletin de la Société Linnéenne de Normandie*, **8**, 101–111.
- GAO, Z. and PENG, D. 2006. The massive gravity flow sediments revealed at Tiwadian outcrop section in southern margin of Ordos Basin. *Journal of Oil & Gas Technology*, **28**, 18–24. [in Chinese]
- GOLUBIC, S. and FOCKE, J. W. 1978. *Phormidium hendersoni* Howe: identity and significance of a modern stromatolite building microorganism. *Journal of Sedimentary Petrology*, **48**, 751–764.
- GUIDO, A., MASTRANDREA, A., ROSSO, A., SANFILIPPO, R., TOSTI, F., RIDING, R. and RUSSO, F. 2014. Commensal symbiosis between agglutinated polychaetes and sulfate-reducing bacteria. *Geobiology*, **12**, 265–275.
- HINDE, G. J. 1887. Review of Bornemann (1886). *Geological Magazine*, **4 Decade III**, 226–229.
- HORODYSKI, R. J. and DONALDSON, J. A. 1980. Microfossils from the Middle Proterozoic Dismal Lakes Group, Arctic Canada. *Precambrian Research*, **11**, 125–159.
- and VONDER HAAR, S. P. 1975. Recent calcareous stromatolites from Laguna Mormona (Baja California) Mexico. *Journal of Sedimentary Petrology*, **45**, 894–906.
- JIANG, H.-X., BAO, H.-P., SUN, L.-Y., WU, Y.-S. and DIAO, J.-B. 2013. Tabulate and rugose corals from the Ordovician reefs in the southern edge of the Ordos Basin and their paleoecology significance. *Acta Palaeontologica Sinica*, **52**, 243–255 [in Chinese with English abstract]
- KLEIN, C., BEUKES, N. J. and SCHOPF, J. W. 1987. Filamentous microfossils in the early Proterozoic Transvaal Supergroup: their morphology, significance, and paleoenvironmental setting. *Precambrian Research*, **36**, 81–94.
- KNOLL, A. H. 1985. Exceptional preservation of photosynthetic organisms in silicified carbonates and silicified peats. *Philosophical Transactions of the Royal Society of London, Series B*, **311**, 111–122.
- and GOLUBIC, S. 1992. Proterozoic and living cyanobacteria. 450–462. In SCHIDLÓWSKI, M., GOLUBIC, S., KIMBERLEY, M. M., McKIRDY, D. M. and TRUDINGER, P. A. (eds). *Early organic evolution: implications for mineral and energy resources*. Springer, 555 pp.
- SWETT, K. and BURKHARDT, E. 1989. Paleoenvironmental distribution of microfossils and stromatolites in the Upper Proterozoic Backlundtoppen Formation, Spitsbergen. *Journal of Paleontology*, **63**, 129–145.
- WÖRNDLE, S. and KAH, L. C. 2013. Covariance of microfossil assemblages and microbialite textures across an Upper Mesoproterozoic carbonate platform. *Palaaios*, **28**, 453–470.
- KORDE, K. B. 1966. Novye materialy k sistematike i evolyutsii krasnykh vodorosley rannego paleozoya. *Doklady Akademii nauk SSSR*, **166**, 1440–1442.
- KRASNOPEEVA, P. S. 1937. Vodorosli i arkeotsiaty drevneyshikh tolshch Potekhinskogo rayona Khakassii. 1–51. In USOV, M. A. (ed.). *Materialy po geologii Krasnoyarskogo kraya*, **3**. West Siberian Geological Trust.
- KRINGS, M., KERP, H., HASS, H., TAYLOR, T. N. and DOTZLER, N. 2007. A filamentous cyanobacterium showing structured colonial growth from the Early Devonian Rhynie chert. *Review of Palaeobotany & Palynology*, **146**, 265–276.
- KUMAR, S. and SRIVASTAVA, P. 1995. Microfossils from the Kheinjua Formation, Mesoproterozoic Semri Group, Newari area, Central India. *Precambrian Research*, **74**, 91–117.
- LI, Z. X. and POWELL, C. M. 2001. An outline of the palaeogeographic evolution of the Australasian region since the beginning of the Neoproterozoic. *Earth-Science Reviews*, **53**, 237–277.
- LIU, L., WU, Y., YANG, H. and RIDING, R. 2016. Ordovician calcified cyanobacteria and associated microfossils from the Tarim Basin, Northwest China: systematics and significance. *Journal of Systematic Palaeontology*, **14**, 183–210.
- MASLOV, V. P. 1956. Iskopaemye izvestkovye vodorosli SSSR. *Trudy Geol Inst SSSR*, **160**, 1–301.
- MATA, S. A., HARWOOD, C. L., CORSETTI, F. A., STORK, N. J., EILERS, K., BERELSON, W. M. and SPEAR, J. R. 2012. Influence of gas production and filament orientation on stromatolite microfabric. *Palaaios*, **27**, 206–219.
- McKENZIE, N. R., HUGHES, N. C., MYROW, P. M., CHOI, D. K. and PARK, T.-Y. 2011. Trilobites and zircons link north China with the eastern Himalaya during the Cambrian. *Geology*, **39**, 591–594.
- MENG, X., GE, M. and TUCKER, M. E. 1997. Sequence stratigraphy, sea-level changes and depositional systems in the Cambro-Ordovician of the North China carbonate platform. *Sedimentary Geology*, **114**, 189–222.
- NICHOLSON, H. A. and ETHERIDGE, R. 1878. *A monograph of the Silurian fossils of the Girvan District in Ayrshire with special reference to those contained in the 'Gray collection', I, vol. 1*. Blackwood, Edinburgh, 341 pp.
- OLIVERI, E., NERI, R., BELLANCA, A. and RIDING, R. 2010. Carbonate stromatolites from a Messinian hypersaline setting in the Caltanissetta Basin, Sicily: petrographic evidence of microbial activity and related stable isotope and REE signatures. *Sedimentology*, **57**, 142–161.
- OTT, E. 1966. Die gesteinsbildenden Kalkalgen im Schlauchkar (Karwendelgebirge). *Jahrbuch des Vereins zum Schütze der Alpenpflanzen und -Tiere*, **31**, 152–159.
- PIA, J., 1927. Abteilung: Thallophyta. 31–136. In HIRMER, M. (ed.). *Handbuch der Paläobotanik, vol. 1*. R. Oldenbourg, Munich.
- POLLOCK, J. B. 1918. Blue-green algae as agents in the deposition of marl in Michigan lakes. *Report of the Michigan Academy of Science*, **20**, 247–260.
- REITLINGER, E. A. 1959. Atlas mikroskopicheskikh organicheskikh ostatkov i problematiki drevnykh tolshch Sibiri. *Trudy Inst Geol Akad Nauk SSSR*, **25**, 1–62.

- RIDING, R. 1975. *Girvanella* and other algae as depth indicators. *Lethaia*, **8**, 173–179.
- 1977. Calcified *Plectonema* (blue-green algae), a recent example of *Girvanella* from Aldabra Atoll. *Palaeontology*, **20**, 33–46.
- 2006. Cyanobacterial calcification, carbon dioxide concentrating mechanisms, and Proterozoic-Cambrian changes in atmospheric composition. *Geobiology*, **4**, 299–316.
- 2012. A hard life for cyanobacteria. *Science*, **336**, 427–428.
- and TOMÁS, S. 2006. Stromatolite reef crusts, Early Cretaceous, Spain: bacterial origin of *in situ*-precipitated peloid microspar? *Sedimentology*, **53**, 23–34.
- and ZHURAVLEV, A. Y. 1995. Structure and diversity of oldest sponge-microbe reefs: Lower Cambrian, Aldan River, Siberia. *Geology*, **23**, 649–652.
- SCHNEIDER, C. A., RASBAND, W. S. and ELICEIRI, K. W. 2012. NIH Image to ImageJ: 25 years of image analysis. *Nature Methods*, **9**, 671–675.
- SCHOPF, J. W. 1968. Microflora of the Bitter Springs Formation, Late Precambrian, central Australia. *Journal of Paleontology*, **42**, 651–688.
- 1996. Metabolic memories of Earth's earliest biosphere. 73–105. In MARSHALL, C. R. and SCHOPF, J. W. (eds). *Evolution and the molecular revolution*. Jones and Bartlett, Boston, 160 pp.
- SEONG-JOO, L. and GOLUBIC, S. 1998. Multi-trichomous cyanobacterial microfossils from the Mesoproterozoic Gaoyuzhuang Formation, China: paleoecological and taxonomic implications. *Lethaia*, **31**, 169–184.
- — 1999. Microfossil populations in the context of syndimentary micrite deposition and acicular carbonate precipitation: Mesoproterozoic Gaoyuzhuang Formation, China. *Precambrian Research*, **96**, 183–208.
- SERGEEV, V. N. 2001. Paleobiology of the Neoproterozoic (Upper Riphean) Shorikha and Burovaya Silicified Microbiotas, Turukhansk Uplift, Siberia. *Journal of Paleontology*, 427–448.
- SHEPARD, R. N. and SUMNER, D. Y. 2010. Undirected motility of filamentous cyanobacteria produces reticulate mats. *Geobiology*, **8**, 179–190.
- SUESS, E., TORRES, M. E., BOHRMANN, G., COLLIER, R. W., GREINERT, J., LINKE, P., REHDER, G., TREHU, A., WALLMANN, K., WINCKLER, G. and ZULEGER, E. 1999. Gas hydrate destabilization: enhanced dewatering, benthic material turnover and large methane plumes at the Cascadia convergent margin. *Earth & Planetary Science Letters*, **170**, 1–15.
- SUN, N., ELIAS, R. J. and LEE, D.-J. 2014. The biological affinity of *Amsassia*: new evidence from the Ordovician of North China. *Palaeontology*, **57**, 1067–1089.
- VISSCHER, P. T., REID, R. P. and BEBOUT, B. M. 2000. Microscale observations of sulfate reduction: Correlation of microbial activity with lithified micritic laminae in modern marine stromatolites. *Geology*, **28**, 919–922.
- WALTER, M. R., BAULD, J. and BROCK, T. D. 1976. Microbiology and morphogenesis of columnar stromatolites (*Conophyton*, *Vacerrilla*) from the hot springs in Yellowstone National Park. 273–310. In WALTER, M. R. (ed.). *Stromatolites*. Developments in Sedimentology, **20**. Elsevier, 790 pp.
- WANG, J., DENG, X., WANG, G. and LI, Y. 2012. Types and biotic successions of Ordovician reefs in China. *Chinese Science Bulletin*, **57**, 1160–1168.
- WEBBY, B. D. 2002. Patterns of Ordovician reef development. 129–179. In KIESSLING, W., FLÜGEL, E. and GOLONKA, J. (eds). *Phanerozoic reef patterns*, **72**. SEPM Special Publication, Tulsa, 735 pp.
- YE, J., YANG, Y. Y., XU, A. D., ZHENG, B. Y., ZUO, Z. F., ZHOU, Y., LI, J. S., LI, Z. X., SONG, G. C. and YONG, Y. X. 1995. *Ordovician reefs in south-western margin Ordos Basin*. Geological Publishing House, Beijing, 80 pp. [in Chinese]
- YUN, Z. 1981. Proterozoic stromatolite microfloras of the Gaoyuzhuang Formation (Early Sinian: Riphean), Hebei, China. *Journal of Paleontology*, **55**, 485–506.